Ultrasound in Med. & Biol., Vol. 29, No. 2, pp. 293–299, 2003

0301-5629/03/$–see front matter

ELSEVIER

doi:10.1016/S0301-5629(02)00707-X

● *Original Contribution*

PRELIMINARY RESULTS USING ULTRASOUND TRANSMISSION FOR IMAGE-GUIDED THERMAL THERAPY

R. L. KING,* G. T. CLEMENT, S. MARUVADA and K. HYNYNEN
Department of Radiology, Brigham and Women's Hospital, Harvard Medical School, Boston, MA, USA

(*Received* 23 *April* 2002; *in final form* 25 *September* 2002)

Abstract—The feasibility of using an acoustic camera as a real-time imaging device for thermal surgery was investigated. The study compares camera images of tissue samples taken before, during and after a volume of tissue was thermally coagulated using focused ultrasound (US). This apparatus has analogous acoustic counterparts to an optical charge couple device (CCD) camera. The setup was operated in transmission mode, with a tissue sample placed between the camera and a 10-MHz illuminating transducer. A high-intensity continuous-wave US signal from a therapeutic transducer was focused inside the sample tissue. A reversible, time-dependent variation in image intensity was observed in the region of the therapeutic sonications in all tissues tested: bovine fat and porcine and rabbit livers. Correlations between image intensities and temperatures were shown; rabbit liver resulted in a correlation coefficient (R^2) of 0.6694 and bovine fat resulted in an R^2 of 0.9455. When temperatures high enough to coagulate tissue were reached, permanent changes in the images were observed. Lesion locations and dimensions from the images were found to be comparable to the sectioned tissue samples. An R^2 of 0.919 resulted when lesion size detected from the camera was compared to the actual lesion size. Preliminary results may indicate that the camera has an application for monitoring thermal surgery. (E-mail: rlking@bwh.harvard.edu) **© 2003 World Federation for Ultrasound in Medicine & Biology.**

Key Words: **Ultrasound, Transmission ultrasound, Ultrasound attenuation, Thermal therapy, Image-guided, Tissue temperature, Acoustic camera.**

INTRODUCTION

Transmission acoustic imaging situates an object between a source and a receiver to provide a linear projection of its attenuation properties. The principle has been applied to develop orthographic images (Fry and Jethwa 1974; Green et al 1973; Hentz et al 1987) and is used in ultrasound (US) transmission tomography (Carson et al 1977; Dines et al 1981; Opielinski and Gudra 2000) to produce 2-D image reconstructions. A modified transmission method, known as reflex transmission imaging (RTI) (Green and Arditi1985; Green et al 1991), uses US backscatter from behind the image plane as a "source," which allows imaging to be performed with a single transducer. A number of studies have revealed the potential of transmission techniques in medical imaging for recording the attenuation properties of varying tissues (Hentz et al 1987; Marich et al 1975a, 1975b; Weigel and Cartee 1983; Wells 2000; Zatz 1975).

Address correspondence to: Randy King, Department of Radiology, Brigham and Women's Hospital, 65 Landsdowne St., Room 252, Cambridge, MA 02139 USA. E-mail: rlking@bwh.harvard.edu

Advances in array technology allow transmission imaging to be performed with high-resolution acoustic cameras. The present study uses an acoustic camera developed by Imperium, Inc. (Lasser et al 1996; Lasser 1997) as an imaging apparatus. It replaces the lens, aperture and sensors of an optical charge couple device (CCD) camera with acoustic counterparts. The camera exploits the similarity in the physical description of optic and acoustic fields, which has prompted the development of numerous acoustic analogs to existing optical systems, such as acoustic holography (Metherell 1968; Metherell et al 1970), lenses (Fjield et al 1997; Lalonde and Hunt 1997) and phase-conjugation (Thomas and Fink 1996). The camera output interfaces with standard video input devices to provide real-time imaging in a specific plane. Others are also studying a variation of this approach, although they are using the camera only as an imaging device and not for thermal monitoring (Ermert et al 2000).

Earlier acoustic camera systems referring to devices that use an acoustic array or scanning laser beam to rapidly detect an ultrasonic image have been described

(Green et al 1973; Metherell et al 1970; Whitman et al 1972). These differ from the contemporary system in both resolution and focusing ability. More recently, systems developed for underwater use (Baikov et al 2000; Erikson et al 1999; Jones 1999) and nondestructive testing (Honda et al 1999) employ a combination of an acoustic lens with new array technologies, but are designed for receiving backscattered signals.

The present study examines the possibility of using transmission imaging to guide thermal therapies. Numerous minimally invasive thermal procedures have been studied as an alternative to surgery and radiation therapy. These procedures require near real-time diagnostic feedback for targeting and monitoring. US (Chapelon et al 1999; Fry et al 1968; ter Harr et al 1989; Sanghvi et al 1999; Sheljaskov et al 1997) computerized tomography (CT) (Fallone et al 1982; Jenne et al 1997) and magnetic resonance imaging (MRI) (Le Bihan et al 1989; Kuroda et al 1992; Parker 1984) have all been tested for thermal exposure monitoring.

We hypothesized that imaging thermally coagulated tissue with transmission US could achieve a higher signal-to-noise ratio (SNR) than backscattered US, due to a strong change in attenuation coefficient (Bamber and Hill 1979; Gertner et al 1997; Damianou et al 1997; Worthington and Sherar 2001) and relatively low change in the reflection coefficient.

We searched for localized change in image intensity due to speed of sound variation caused by temperature changes; thus, allowing the US focal region to be identified.

Specifically, we tested the transmission method with the acoustic camera system for 1. its ability to image coagulated tissue, 2. the sensitivity to temperature elevation at the focus of a therapeutic US field in *ex vivo* tissue samples during sonication, and 3. the correlation between image intensity and tissue temperature.

MATERIALS AND METHODS

A prototype US camera (Lasser 1997) was used for the experiments. The system uses a planar radiator, separated by a distance of 23.5 cm from the camera, to illuminate a region of the target tissue. The planar illuminating transducer was a single-element piezoelectric (PZT) transducer with a matching layer, a center frequency of 7.5 MHz, and 4.5 cm^2. An illustration of this system is shown in Fig. 1. US scattered by the target is focused onto the camera image plane using a compound system of acoustic lenses. If the target is relatively homogeneous relative to the signal frequency, scattering may be neglected and the image will be a product of the attenuation and phase distortion in the camera's object plane (Fig. 1).

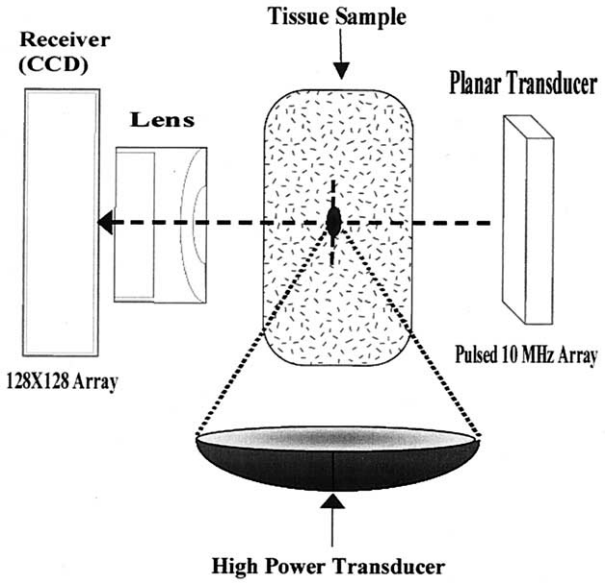

Fig. 1. Acoustic camera transmission system diagram.

The camera's image plane consists of PVDF (polyvinylidene difluoride) piezoelectric material 1 cm^2 divided into 128 $\times$ 128 active pixel elements with .085 mm center-to-center spacing deposited upon a standard silicon readout CCD multiplexer. The PVDF array is sensitive over a bandwidth of more than 20 MHz. Use of a standardized chip allows interfacing with commercial video and data-acquisition equipment. Moving the lens on the camera, which is adjusted similarly to an optical camera, chooses the object plane. Feedback is provided from real-time video images. Video was fed to a 500-MHz PC outfitted with Pinnacle DV 500 frame grabber (Pinnacle Systems, Inc., Mountain View, CA). Still images were obtained in a bitmap format using the Acoustocam imaging software (Imperium, Inc., Silver Spring, MD) and movies were recorded using Adobe Premiere 5.1C.

The signal transducer and receiving array were tested to measure the camera's sensitivity, field-of-view (FOV), therapeutic focus and lesion-detection capability and SNR. The driving system supplied a 10-MHz impulse to the source transducer with a variable peak voltage of between 210 V to 710 V, as selected by the gain control on the camera. The measurements were conducted in a tank filled with degassed deionized water and padded with rubber to inhibit reflections from the tank walls.

To test the camera's ability to image small features, polystyrene phantoms were created, as shown in Fig. 2. The first (Fig. 2a) was a 5-mm thick plate containing four holes whose diameters were 3.2 mm, 1.59 mm, 0.78 mm and 0.4 mm. The phantom was imaged (Fig. 2b) and

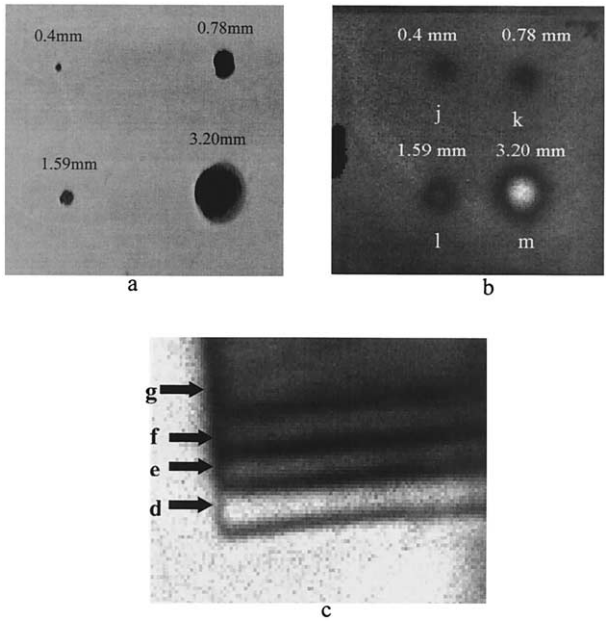

Fig. 2. (a) Photograph of 0.5-mm thick polystyrene phantom with hole diameters of 0.4 mm, 0.78 mm, 1.59 mm and 3.20 mm as measured with calipers. (b) Average measured diameters from the acoustic camera transmission image of a 5.0-mm thick polystyrene phantom, (j) 0.75 mm ± 0.12 mm, (k) 1.1 mm ± 0.19 mm, (l) 1.42 mm ± 0.25 mm and (m) 3.49 mm ± 0.21 mm. (c) Acoustic camera transmission image of polystyrene phantom with varying thickness of (d) 0.5 mm, (e) 1.64 mm, (f) 2.90 mm and (g) 4.30 mm with normalized intensities of (d) 0.94, (e) 0.50, (f) 0.35 and (g) 0.28.

measurements of the features were made using the measurement program, which calibrated a number of pixels to a scale.

The second phantom (Fig. 2c) was a polystyrene plate with thickness steps of (Fig. 2d) 0.5 mm, (Fig. 2e) 1.64 mm, (Fig. 2f) 2.90 mm and (Fig. 2g) 4.30 mm.

With the source planar transducer positioned 23.5 cm from the camera array, as depicted in Fig. 1, FOV measurements were obtained as a function of position. The measurements were obtained by focusing the camera on a metal grating placed at varying positions between the source and receiver. At each location, an image was acquired. Images from the camera were calibrated to give the FOV at a particular location on the camera axis.

Three tissue types, bovine fat, rabbit liver and porcine liver, were used to detect temperature and intensity changes. Sonications varied in power levels and duration. The rabbit and porcine liver tissues were chosen due the ability to obtain these tissues fresh. Immediately after euthanizing the animal, the porcine and rabbit livers were removed and placed in 0.9% sodium chloride solution and degassed at −1.0 bar for approximately 1 h and used in the experiments that same day. The bovine fat, obtained from a local butcher due to the quantity needed, was also degassed at −1.0 bar in 0.9% sodium chloride solution for approximately 1 h, and used the same day it was obtained. All samples were less than 5-cm thick. A bare junction copper-constantan thermocouple, with wire diameter 0.05 mm, was inserted into the tissue using a catheter and positioned directly in the focus of the high-intensity therapeutic transducer by sonicating at 1.0 W while moving the tissue until a maximum temp reading was found. A 10-s baseline reading from the thermocouple was obtained before the treatment sonications, during which the temperature of the tissue volume was recorded. Sonications performed with the thermocouple varied in power levels, 1 to 50 W, and duration, 5 to 10 s.

Tissue samples were placed in the camera's image plane, as shown in Fig. 1. A focused transducer was placed perpendicular to the camera's axis with its focus within the camera's FOV. In separate experiments, an air-backed 1.1-MHz, 10-cm diameter PZT transducer and a tungsten-backed 1.8-cm diameter 2.0-MHz transducer were used. The air-backed transducer was impedance matched to electrical resonance at 50 Ω to assure maximum power output to the transducer from a multichannel amplifier system constructed in-house (Daum et al 1998). The 2-MHz tungsten-backed transducer input was a continuous-wave (CW) sinusoid generated by an arbitrary waveform generator (Wavetek, San Diego, CA; model 305) and fed to a power amplifier (ENI, Rochester, NY; model 3100L).

Images were recorded with the camera before, during and after high-intensity US was focused into the tissue. Sonications were performed at low and high power to induce tissue temperatures below and above the coagulation threshold. Low power sonications were used to detect the focus at temperatures too low to cause physiologic changes to the tissues. Higher temperatures, achieved by using higher input powers and longer sonication times, were used to image coagulated tissue. Over the sonication period, the temperature at the US focus was recorded using a thermocouple. The temperature data were read by a multimeter (Keithley Instruments, Cleveland, OH; model 2700).

RESULTS

The first plate had four holes with diameters of 0.4 mm, 0.78 mm, 1.59 mm and 3.20 mm (Fig 2a). All the holes were seen as reduced signal intensity, except the two largest holes, which showed an increase in the centers (Fig. 2b). A total of 10 measurements of each diameter were taken across the images. The average visually detected diameters of the holes in the images was usually larger than the actual diameters of the holes as measured by calipers. The one hole that measured smaller on the

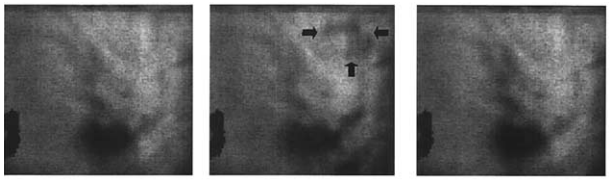

Fig. 3. US focus in pig liver. (a) Baseline before sonication, (b) immediately after 20-W 20-s sonication and (c) 120 s after sonication. Arrows outline heating. The FOV on these images is approximately 3 cm × 3.5 cm.

acoustic camera image compared to the real size was still within 1 SD (Fig. 2j). The percent difference between the actual diameters and the diameters measured from the acoustic camera images increased with decreasing radius, giving differences of 9%, 11%, 34% and 61%; the larger errors occurred below 1 mm (Fig. 2).

With the second phantom (Fig. 2c), the signal intensity decreased with the increasing thickness of the phantom. Acoustic camera transmission image of a polystyrene phantom (Fig. 2c) with varying thickness of (Fig. 2d) 0.5 mm, (Fig. 2e) 1.64 mm, (Fig. 2f) 2.90 mm and (Fig. 2g) 4.30 mm with normalized intensities of (Fig. 2d) 0.94, (Fig. 2e) 0.50, (Fig. 2f) 0.35 and (Fig. 2g) 0.28, corresponded to increasing thickness.

When sonications of the tissue samples were performed at low powers, reversible image intensity changes were observed. In all types of tissue, an intensity change was seen at all power levels and durations. Figure 3, with an FOV of approximately 3 cm × 3.5 cm, illustrates an example of the intensity change and fallback to baseline in porcine liver sonicated at 14.4 W for 30 s.

Correlation of the image intensity with thermocouple measurements is illustrated in Fig. 4 for one experiment in rabbit liver and bovine fat. Also shown are the time relationships for thermal and intensity data. Figure 5 shows the mean signal intensities and thermocouple readings for all the liver ($n = 5$) and fat ($n = 12$) experiments. Each data point in Fig. 5a is a mean intensity value of points within a 1° range. In Fig. 5b, each data point is a mean intensity value of points within a 5° range. The region-of-interest (ROI) is one pixel chosen within the heated region. Initial temperature for all experiments was room temperature. Intensity information from the camera images could not be obtained while sonicating with the therapeutic transducer due to disruption of the source signal. With the liver samples, lower powers were used to avoid coagulation as opposed to the fat samples, which allowed the use of higher sonicating powers. The higher powers resulted in a normalized

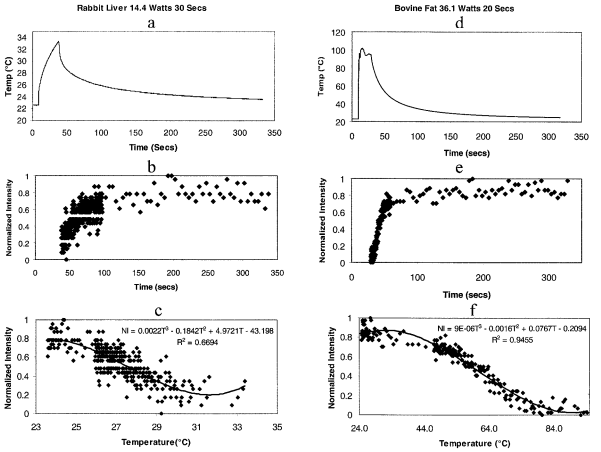

Fig. 4. Thermocouple measurements over time in (a) rabbit liver and (d) bovine fat. (b), (e) Normalized intensity (NI) from the acoustic camera images over time for the two tissue types. (c), (f) NI from the acoustic camera correlated to thermocouple temperatures. R^2 = correlation coefficient.

intensity close to zero, immediately after the sonocation, at the focus.

Images before and after a high-power sonication with a therapeutic transducer in porcine liver are shown in Fig. 6 and compared to a photograph of the same lesion. In all cases, when coagulation of the tissue was observed, the signal intensity at the sonicated location decreased. A mean contrast-to-noise (CNR) of 10.7 was observed when the camera source was operated at midrange intensity. At high intensity, the CNR dropped to a mean value of 3.2 when measuring the lesions. The CNR was sampled from a region in the tissue near the heating. The ROI varied with each sonication, but was limited to an area smaller than the heated region. The lesion diameters measured from the images ($n = 12$) displayed good linear correlation with the actual lesion size measured from gross inspection, shown in the plot in Fig. 7. The fat samples did not show a similar reduction in the signal intensity after the sample temperatures returned to baseline.

The correlation of the signal intensity values for the liver samples before and after treatment with focused US was compared with the thickness of the sample. The samples were imaged at 10 MHz. The resulting increase in the attenuation coefficient for the samples ($n = 5$) was found to be 0.35 Np cm^{-1} at 10 MHz with a slope of 0.0351.

DISCUSSION

This study tested the use of a new US transmission camera for the monitoring of focused US thermal surgery. The results demonstrated that the transmission US

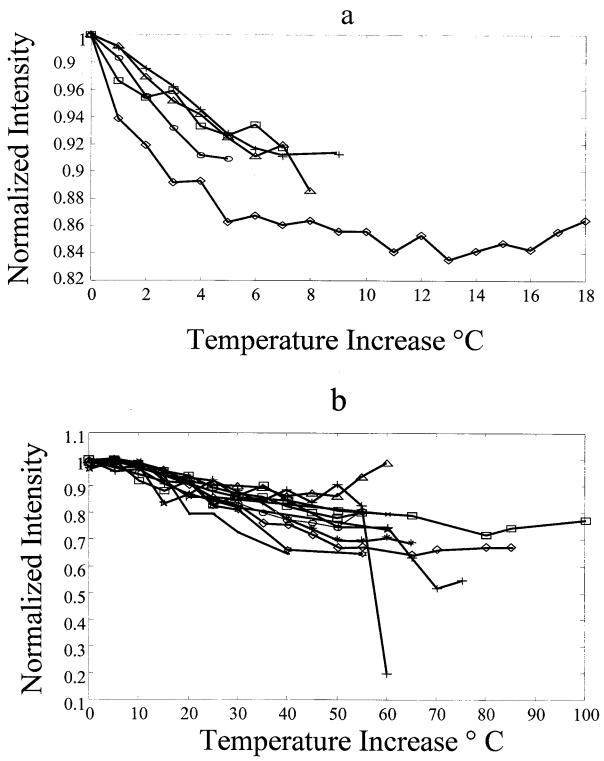

Fig. 5. (a) Mean signal intensities and temperature change readings from the thermocouple for all the liver experiments (n = 5). (b) Mean signal intensities and temperature change readings from the thermocouple for all the fat experiments (n = 12).

camera had the spatial resolution and sensitivity to attenuation changes to be able to detect thermally coagulated tissue volumes. In addition, small temperature elevations induced at the focus of a therapeutic US beam were visible, allowing the focal location to be detected before thermally coagulating the tissue volume. Both of these features are valuable for guiding and monitoring focused US surgery and, thus, the US transmission camera may have a role in monitoring US surgery and other

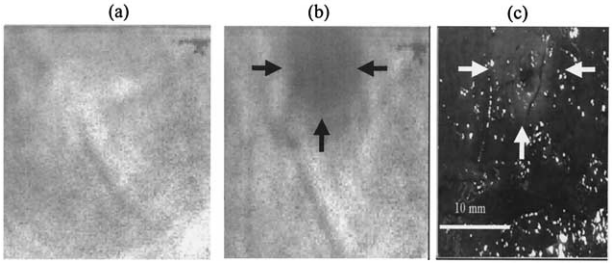

Fig. 6. Acoustocam image of porcine liver (a) before and (b) after high-intensity sonications compared with (c) cross-section photograph of the coagulated lesion. Arrows outline lesion.

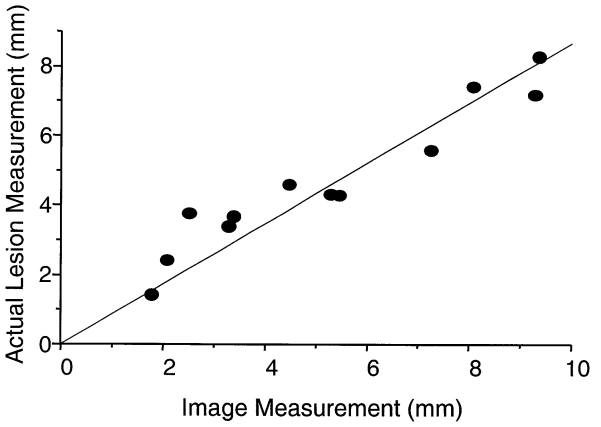

Fig. 7. Actual lesion size from gross inspection, correlated with lesion size as measured with the acoustic camera.

thermal therapies in sites that allow US transmission, such as the breast.

The experiments with the polystyrene plate, chosen because it is a readily available, rigid material that offers different sound speed and attenuation properties from those of water, demonstrated that submillimeter-diameter volumes of material with different acoustic speed and attenuation could be detected. The smallest holes in the plate showed decreased signal intensity with a larger diameter than the physical size of the hole. This is most likely caused by the distortion of the wave due to the difference in the sound speed in the water (1500 m/s) and the polystyrene (2200 m/s) (Hung and Goldstein 1983). This distortion causes the waves to destructively interfere with the remaining wave at the detector. The largest hole showed an increased signal intensity in the middle, corresponding to the smaller attenuation in water (20° 25E-3 Np cm/MHz) (Duck 1990) when compared with the polystyrene (18.76 Np cm/Mhz) (Hung and Goldstein 1983). This increased signal area was surrounded by a ring of reduced signal, again correlating with the diffraction of the waves. Structures, such as bone, with varying acoustic speeds and attenuations from that of tissue could be detected with the camera system.

Small temperature elevations on the order of 1 °C were visually quantitated with the camera in both liver and fat, and the changes in intensities at low temperatures can be seen in Fig. 5. The temperature increase caused a change in the US propagation speed in the heated volume. The increase or decrease in the speed of sound causes the wavefront to bend, inducing the waves to arrive out of phase to the detector; thus, inducing a decrease in the signal intensity. This explains why both the liver and fat had a reduction in the signal intensity even though the temperature coefficient in fat is negative and in liver is positive (Bamber and Hill 1979). The

slopes of different tissues vary;bovine fat at 20°C (−10.1 ms °C) (Bamber and Hill 1979) and bovine liver at 20°C (1.01 m s °C) (Bamber and Hill 1979); thus, it is expected that this signal could not be an accurate measure of the peak temperature. However, it could be used to localize the focus.

The thermal coagulation of liver tissue has been shown to increase the tissue attenuation (Bevan et al 2001; Damianou et al 1997; Duck 1990) and, thus, the coagulated volume should show as a reduced signal area in the image. The speed of sound in the coagulated tissue has been reported to remain approximately unchanged (Duck 1990), indicating that the ring effects seen with the polystyrene plate would not be present. Our experiments with the liver verified this assumption, showing a reduction in the signal intensity that depended on the coagulated tissue volume. The attenuation was calculated using the baseline intensity, the attenuated intensity and the thickness of the lesion, to determine the attenuation coefficient. The results indicated an average attenuation coefficient increase of 0.35 Np cm at 10 MHz. This is roughly equal to the attenuation of US in liver (0.34 Np cm/MHz) (Duck 1990) and, thus, indicates that the attenuation of the coagulated liver has roughly doubled. This agrees well with the published literature (Damianou et al 1997; Gerter et al 1997). Coagulated tissue volumes as seen on the camera images can underestimate the actual lesion volume in which cell death occurs. The damage could take days to become manifest, illustrating one of the limitations of attenuation-sensitive imaging. A histologic study of the damaged area would be needed to confirm the camera's precision in determining exact lesion boundaries.

SUMMARY

The newly developed US transmission camera shows promise for monitoring focused US thermal surgery in organs that would allow US transmission. However, more work needs to be done to verify the findings *in vivo* and with tumor tissues to determine if the method is sensitive enough to be useful in more clinically relevant settings.

Acknowledgments—This work was supported by the NIH (grant CA46627).

REFERENCES

Baikov SV, Svet VD, Sizov VI. Experimental investigation of the resolution and sensitivity of an ultrasonic imaging camera with an immersion lens. Acoust Phys 2000;46:518–522.

Bamber JC, Hill CR. Ultrasonic attenuation and propagation speed in mammalian tissues as a function of temperature. Ultrasound Med Biol 1979;4:149–157.

Bevan PD, Sherar MD. B-scan ultrasound imaging of thermal coagulation in bovine liver: Frequency shift attenuation mapping. Ultrasound Med Biol 2001;27:809–817.

Carson PL, Oughton TV, Hendee WR, Ahuja AS. Imaging soft tissue through bone with ultrasound transmission tomography by reconstruction. Med Phys (USA) 1977;4:302.

Chapelon JY, Ribault M, Vernier F, Souchon R, Gelet A. Treatment of localised prostate cancer with transrectal high intensity focused ultrasound. Eur J Ultrasound 1999;9:31–38.

Damianou CA, Sanghvi NT, Fry FJ, Maass-Moreno R. Dependence of ultrasonic attenuation and absorption in dog soft tissue on temperature and thermal dose. Acoust Soc Am 1997:628–634.

Daum D, Buchanan M, Fjield T, Hynynen K. Design and evaluation of a feedback based phased array system for ultrasound surgery. IEEE Trans Ultrason Ferroelec Freq Control 1998;45:431–438.

Dines KA, Fry FJ, Patrick JT, Gilmor RL. Computerized ultrasound tomography of the human head: Experimental results. Ultrason Imaging 1981;3:342–351.

Duck F. Physical properties of tissue a comprehensive reference book. London: Academic Press, 1990.

Erikson K, Stockwell J, Hairston A, et al. Information systems for Navy divers and autonomous underwater vehicles operating in very shallow water and surf zones. Proc SPIE 1999;3711:33–42.

Ermert H, Keitmann O, Oppelt R, et al. A new concept for a real-time ultrasound transmission camera. IEEE Ultrasonics Symposium, 2000.

Fallone BG, Moran PR, Podgorsak EB. Noninvasive thermometry with a clinical x-ray CT scanner. Med Phys 1982;9:715–721.

Fjield T, Sorrentino V, Cline H, Hynynen K. Design and experimental verification of thin acoustic lenses for the coagulation of large tissue volumes. Phys Med Biol 1997;42:2341–2354.

Fry FJ, Jethwa CP. Ultrasonic transmission imaging using gaussian noise source. J Clin Ultrasound 1974;2:230.

Fry WJ, Leichner GH, Okuyama D, Fry FJ, Fry EK. Ultrasonic visualization system employing new scanning and presentation methods. J Acoust Soc Am 1968;44:1324–1338.

Green PS, Arditi M. Ultrasonic reflex imaging. Ultrason Imaging (USA) 1985;7:201–214.

Green PS, Ostrem JS, Whitehurst TK. Combined reflection and transmission ultrasound imaging. Ultrasound Med Biol (UK) 1991;17: 283–289.

Green PS, Schaefer LF, Jones ED, Suarez JR. A new high-performance ultrasonic camera. In: Green PS, ed. Acoustical holography. New York: Plenum Press, 1973.

Hentz VR, Green PS, Arditi M. Imaging studies of the cadaver hand using transmission ultrasound. Skeletal Radiol 1987;16:474–480.

Honda T, Honda Y, Ikeda M, Nakajima M. Quasi-real time imaging using ultrasonic Fourier camera. Trans Inst Electron Inf Commun Eng 1999;J82-A:201–208.

Hung B, Goldstein A. Acoustic parameters of commercial plastics. IEEE Trans Sonics Ultrason 1983;SU-30(4):249–254.

Jenne JW, Bahner M, Spoo J, et al. CT on-line monitoring of HIFU therapy. 1997 IEEE Ultrasonics Symposium Proceedings. An International Symposium (Cat. No. 97CH36118). 1997:1377.

Jones ISF. High resolution underwater acoustic imaging. Oceans 99 MTS/IEEE Proc 1999;3:1093–1097.

Kuroda K, Abe K, Tsutsumi S. Non-invasive temperature mapping based on NMR procedure. In: Diller K, Shitzer A, ed.s. Macroscopic and microscopic heat and mass transfer in biomedical engineering. Belgrade: International Center for Heat and Mass Transfer, 1992:199–217.

Lalonde R, Hunt JW. Variable frequency field conjugate lenses for ultrasound hyperthermia. IEEE Trans Ultrason Ferroelec Freq Control 1997;42:825–831.

Lasser ME. A novel high speed, high resolution, ultrasound imaging system. Materials Research Society Symposium Proceedings Series, 1997:503.

Lasser ME, Harrison GH, Agarwal M. Acoustic microscopy for 100% non-destructive semiconductor package evaluation. Proceedings of the 1996 International Symposium on Microelectronics, 1996:82–86.

Le Bihan D, Delannoy J, Levin RL. Temperature mapping with MR imaging of molecular diffusion: Application to hyperthermia. Radiology 1989;171:853–857.

Marich KW, Zatz LM, Green PS, Suarez JR, Macovski A. Real-time imaging with a new ultrasonic camera: Part I, In vitro experimental studies on transmission imaging of biological structures. J Clin Ultrasound 1975a;3:5–16.

Marich KW, Zatz LM, Green PS, Suarez JR, Macovski A. Real-time imaging with a new ultrasonic camera: Part II, Studies in normal adults. J Clin Ultrasound 1975b;3:17–22.

Metherell AF. Holography with sound. Science J 1968;4:57–62.

Metherell AF, Spinak S, Pisa EJ. Temporal reference acoustic holography. Proceedings of the 2nd International Symposium on Acoustical Holography, 1970:69–86.

Opielinski KJ, Gudra T. Ultrasound transmission tomography image distortions caused by the refraction effect. Ultrasonics 2000;38: 424–429.

Parker DL. Applications of NMR imaging in hyperthermia: An evaluation of the potential for localized tissue heating and noninvasive temperature monitoring. IEEE Trans Biomed Eng 1984;31:161–167.

Sanghvi NT, Foster RS, Bihrle R, et al. Noninvasive surgery of prostate tissue by high intensity focused ultrasound: An updated report. Eur J Ultrasound 1999;9:19–29.

Sheljaskov T, Lerch R, Fuchs A, Schatzle U. A phased array antenna for simultaneous thermotherapy and sonography. 1997 IEEE Ultrasonics Symposium Proceedings. An International Symposium (Cat.No.97CH36118). 1997:1701.

ter Haar G, Sinnett D, Rivens I. High intensity focused ultrasound—a surgical technique for the treatment of discrete liver tumors. Phys Med Biol 1989;34:1743–1750.

Thomas J-L, Fink MA. UItrasonic beam focusing through tissue inhomogeneities with a time reversal mirror: Application to transskull therapy. IEEE Trans Ultrason Ferroelec Freq Control 1996;43: 1122–1129.

Weigel JP, Cartee RE. Preliminary study on the use of ultrasonic transmission imaging to evaluate the hip joint in the immature dog. Ultrasound Med Biol (UK) 1983;9:371–378.

Wells PNT. Advances in ultrasound: From microscanning to telerobotics. Br J Radiol 2000;73:1138–1147.

Whitman RL, Korpel A, Ahmed M. Novel technique for real-time depth-gated acoustic image holography. Appl Phys Lett 1972;20: 370–371.

Zatz LM. Initial clinical evaluation of a new ultrasonic camera. Radiology 1975;117:399–404.